J Mater Sci: Mater Med (2008) 19:479–484
DOI 10.1007/s10856-006-0028-7

Effect of molding pressure on fabrication of low-crystalline calcite block

Xin Lin · Shigeki Matsuya · Masaharu Nakagawa · Yoshihiro Terada · Kunio Ishikawa

Received: 4 July 2006 / Accepted: 19 October 2006 / Published online: 3 July 2007

Abstract We have reported that low-crystalline porous calcite block, which is useful as a bone substitute or a source material to prepare apatite-type bone fillers could be fabricated by exposing calcium hydroxide compact to carbon dioxide gas saturated with water vapor. In the present study, we investigated the effect of molding pressure on the transformation of calcium hydroxide into calcite and the mechanical strength of the carbonated compact. Transformation into calcite was almost completed within 72 h, however, a small amount of $Ca(OH)_2$ still remained unreacted at higher molding pressure because of incomplete penetration of CO_2 gas into the interparticle space due to dense packing of $Ca(OH)_2$ particles. On the other hand, high molding pressure resulted in an increase in diametral tensile strength (DTS) of the calcite compact formed. Critical porosity of the calcite block was calculated as approximately 68%.

Introduction

Calcium carbonate ($CaCO_3$) has been used as bone filler for the reconstruction of bone defects and as a source material for bone fillers. Marine coral is made of aragonite-type calcium carbonate (>97%). The coral has been clinically used as bone substitute in dental, maxillo-facial, cranio-facial, and orthopedic surgeries for the reconstruction of bone defects [1–5]. The coral is also used as a source material to prepare apatite-type bone fillers. When the coral is hydrothermally treated in diammonium hydrogen phosphate solution, it transforms into apatitic mineral without changing its morphology. The bone filler is called coralline apatite and has been clinically used as a bone substitute in the United States [6–9]. However, the usage of the coral is limited due to its high cost and serious environmental problems. Moreover, the collected coral have to be cleaned to prevent inflammatory reaction caused by proteins and other elements present as impurities. Drawbacks of the coral mentioned above would be solved if calcium carbonate compact can be prepared artificially. Though the sintering of calcium carbonate powder results in calcium carbonate block, it would cause liberation of carbon dioxide and formation of calcium oxide above 650 °C. In addition, calcium carbonate with extremely high crystallinity is obtained even when low crystalline calcium carbonate powder is used. Unfortunately, formation of calcium oxide and high-crystalline calcium carbonate is not desirable with respect to tissue response and resorbability, when it is used as the bone substitute.

In our previous study [10], therefore, we proposed a fabrication method of pure, low-crystalline calcite compact with adequate and high mechanical strength calcium carbonate (calcite) compact by carbonation of calcium hydroxide ($Ca(OH)_2$) compact in CO_2 stream saturated with water vapor. We found that development of DTS proceeded in two stage, which corresponded to rapid carbonation at the surface of the $Ca(OH)_2$ particle and

X. Lin · M. Nakagawa · K. Ishikawa
Department of Biomaterials, Faculty of Dental Science, Kyushu University, 3-1-1 Maidashi, Higashi-ku, Fukuoka 812-8582, Japan

X. Lin · Y. Terada
Department of Fixed Prosthodontics, Faculty of Dental Science, Kyushu University, Fukuoka, Japan

S. Matsuya (✉)
Section of Bioengineering, Department of Dental Engineering, Fukuoka Dental College, Sawara-ku, Fukuoka 814-0193, Japan
e-mail: smatsuya@college.fdcnet.ac.jp

diffusion process through the calcite layer at the surface to complete carbonation. It was considered that DTS before and after carbonation depended on the molding pressure used.

In the present study, we investigated the formation process and measured DTS of calcite compact prepared by carbonation of $Ca(OH)_2$ compact under wider range of molding pressure. The aim of this investigation was to clarify the effect of molding pressure on mechanical strength and to get more information about the fabrication process of calcite compact as a bone substitute and/or as a precursor for apatite block.

Materials and methods

Calcium hydroxide compact preparation

Commercially available calcium hydroxide ($Ca(OH)_2$, Wako Chemicals, Tokyo, Japan) was used in this study. The $Ca(OH)_2$ powder, 0.2 g, was placed in a stainless steel mold and pressed uniaxially with an oil pressure press machine (Riken Power, Riken Seiki, Japan) under 1–15 MPa pressure. Specimens prepared were 10 mm in diameter and 1–3 mm in height.

Carbonation of $Ca(OH)_2$ compact

The prepared $Ca(OH)_2$ compacts were placed in a reaction vessel saturated with water vapor at room temperature. Carbon dioxide gas was introduced in the vessel at a flow rate of 0.15–0.20 L/min and the $Ca(OH)_2$ compacts were carbonated up to 72 h.

Mechanical testing

After the carbonation for the prescribed periods, mechanical strength of the specimens was evaluated in terms of diametral tensile strength (DTS). The specimens were crushed using a universal testing machine (IS5000, Shimadzu Co., Kyoto, Japan) at a cross-head speed of 1 mm/min after measuring the diameter and height of each specimen with a micrometer (156-101, Mitutoyo Co. Ltd., Kanagawa, Japan). The DTS values were averaged over at least eight specimens.

Microstructure

Morphology of the fractured surface of the specimen was characterized by means of a scanning electron microscope (SEM, JSM 5400LV, JEOL Co. Ltd., Tokyo, Japan) at 15 kV of accelerating voltage after gold sputter coating.

X-ray diffraction analysis

The specimens ground into fine powders were characterized by X-ray diffraction (XRD) analysis. The XRD patterns were recorded with a vertically mounted diffractometer system (RIGAKU RINT 2500V, Tokyo, Japan) using counter-monochromatized CuK_α radiation generated at 40 kV and 100 mA. The specimens were scanned from 3° to 60° 2θ (where θ is the Bragg angle) in a continuous mode at a scanning rate of 2°/min. Quantitative analysis was also done on the specimens during carbonation. Calibration curve for the quantitative analysis was made using separated diffraction peaks of $Ca(OH)_2$ (0 0 1, d = 4.905 Å) and calcite (0 –2 2, d = 2.095 Å) respectively. Crystallite sizes, D of the calcite formed by carbonation for 72 h of $Ca(OH)_2$ compact prepared at various molding pressures were calculated based on XRD analysis.

The following relation holds between half width (β) and crystallite size (D).

$$\beta \cdot \cos(\theta) = K\lambda/D$$

where θ and λ are Bragg angle and wave length of X-ray (CuK_α) used, respectively. After β was corrected for the instrumental broadening by using well crystallized α-quartz heated at 1,050 °C, crystallite size was calculated based on the above equation.

Porosity measurement

For porosity measurement, the apparent density of specimen before and after carbonation was calculated from the specimen's weight and dimensions. The theoretical densities of pure calcium hydroxide (2.24 g/cm^3) and calcite (2.711 g/cm^3) were used for the calculation. As a small amount of calcium hydroxide still remained after the carbonation, its content was taken into account for the apparent density calculation. Relative density was calculated from a ratio of the apparent density to the theoretical density. The total porosity of specimen is then defined as

$$\text{Total porosity}\ (\%) = 100\ (\%) - \text{Relative density}\ (\%)$$

Total porosity was averaged over at least five specimens.

Results

Figure 1 shows the X-ray diffraction patterns of calcium hydroxide compacts prepared at 2 MPa (A) and 15 MPa (B) and treated with CO_2 gas for up to 72 h. In each figure, a diffraction pattern of the sample (a) before carbonation

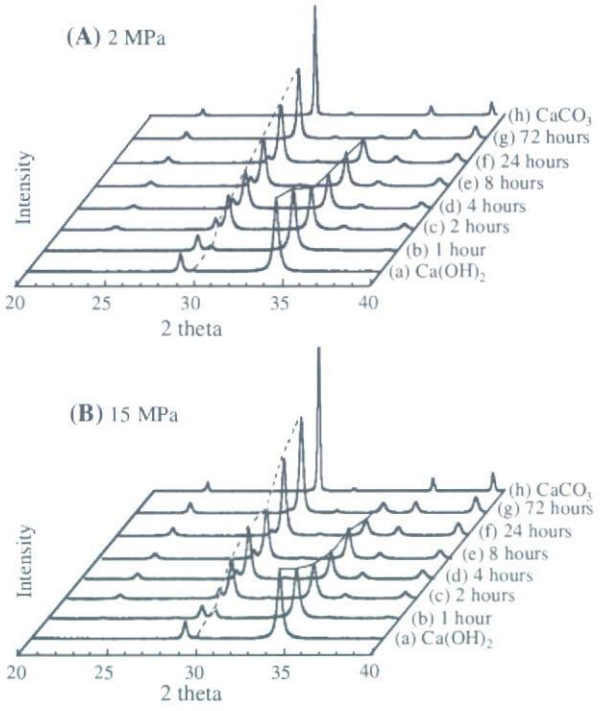

Fig. 1 X-ray diffraction patterns of calcium hydroxide compacts prepared at (**A**) 2 MPa and (**B**) 15 MPa treated with CO_2 gas for different time periods. In each figure, a diffraction pattern of the sample (a) before carbonation and (h) commercially contained calcite powder were also included for comparison. Specimens were treated with CO_2 gas for (b) 1 h, (c) 2 h, (d) 4 h, (e) 8 h, (f) 24 h, and (g) 72 h respectively

and (h) commercially contained calcite powder were also included for comparison. Specimens were treated with CO_2 gas for (b) 1 h, (c) 2 h, (d) 4 h, (e) 8 h, (f) 24 h, and (g) 72 h, respectively. As shown in this figure, the intensities of peaks attributed to calcium hydroxide, $2\theta = 28.7$ (0 –1 0) and $2\theta = 34.1$ (0 1 1), decreased gradually with time and meantime the intensities of peaks attributed to calcite, $2\theta = 29.4$ (0 –1 –4) and $2\theta = 36.0$ (1 1 0) appeared and their intensities increased with time in both cases. In the case of other molding pressures, the change in XRD patterns was quite similar though the data are not shown.

Table 1 Changes in the amount of calcite phase in the compacts with time at various molding pressures

Molding pressure (MPa)	$CaCO_3$ (wt%)
1	99.8
2	97.7
3	97.2
5	98.5
7.5	92.8
10	90.1
15	86.3

Table 1 shows the amount of calcite formed after carbonation for 72 h at various molding pressure. As shown in this table, the amount of calcite varied between 86.3 wt% and 99.8 wt% and tended to decrease with increasing the molding pressure.

Table 2 summarizes crystallite size, D of the calcite formed by carbonation for 72 h of $Ca(OH)_2$ compact prepared at various molding pressures. Crystallite size of the initial calcium hydroxide powder was 30.2 nm. As can be seen in this table, crystallite size increased with molding pressure to reach 46.8 nm when compacted at 15 MPa. It should be noted that crystallite size of the calcite formed by the carbonation was much smaller than that of the commercial one (83.4 nm).

Figure 2 shows the SEM images of the fractured surfaces of calcium hydroxide compacts prepared at various molding pressures before carbonation (left column; (a)–(e)) and after carbonation for 72 h (right column; (f)–(i)), respectively. The original $Ca(OH)_2$ powder had particle size ranging from sub micron to several microns with an irregular shape. We found no remarkable differences in the surface structure before and after the carbonation for 72 h as shown in Fig. 2, nevertheless X-ray diffraction analysis showed that approximately 86–100 wt% of $Ca(OH)_2$ had transformed into calcite depending on the molding pressure.

Figure 3 shows the change in porosity of $Ca(OH)_2$ compact before and after carbonation for 72 h as a function of molding pressure. The porosity decreased with increase in molding pressure in spite of carbonation. Porosity after the carbonation was approximately 4% smaller than that before carbonation regardless of the molding pressure.

Figure 4 shows the change in DTS values of $Ca(OH)_2$ compacts prepared at various molding pressures as a function of carbonation time. Irrespective of the molding pressure, DTS values rapidly increased with time within

Table 2 Comparisons of crystallite size, D for each compact formed by carbonation for 72 h of $Ca(OH)_2$ compact prepared at various molding pressures

Molding pressure (MPa)	Crystallite size (nm)
Initial calcium hydroxide powder	30.2
1	35.5
2	36.9
3	35.2
5	35.3
7.5	42.3
10	45.1
15	46.8
commercial calcite powder	83.4

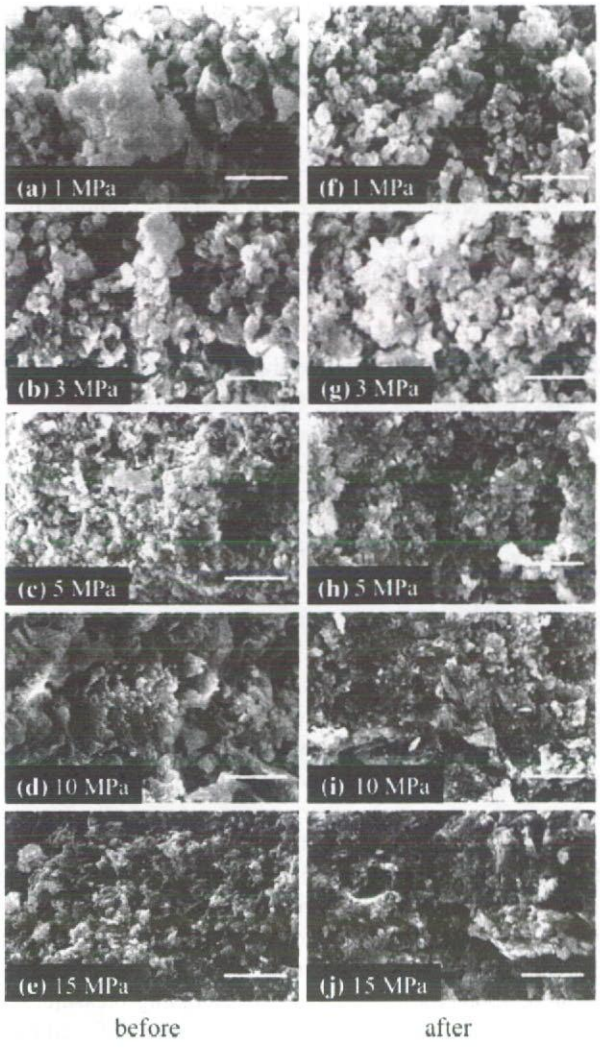

Fig. 2 Typical scanning electron micrographs of the fractured surfaces of $Ca(OH)_2$ compacts prepared at (**a**) and (**f**) 1 MPa; (**b**) and (**g**) 3 MPa; (**c**) and (**h**) 5 MPa; (**d**) and (**i**) 10 MPa; (**e**) and (**j**) 15 MPa before carbonation (left column) and after carbonation for 72 h (right column). Bar: 5 μm

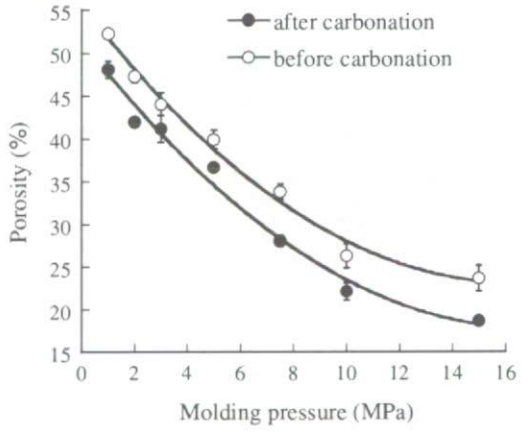

Fig. 3 Change in porosity of $Ca(OH)_2$ compacts prepared at various molding pressures before and after carbonated for 72 h. The bars in the figure denote standard deviation

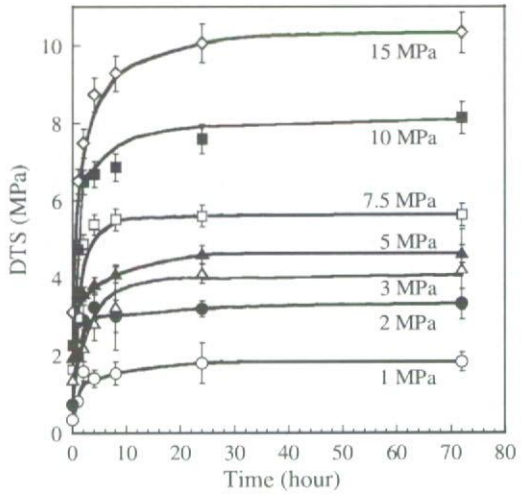

Fig. 4 Change in DTS values of $Ca(OH)_2$ compacts prepared at various molding pressures as a function of carbonation time. The bars in the figure denote standard deviation

first several hours and a prolonged carbonation after 24 h gave only a slight increase in DTS values. Higher molding pressure resulted in a higher DTS value after 72 h of carbonation.

Figure 5 shows DTS values after carbonation for 72 h plotted against molding pressure. DTS values of the green compact before carbonation are also plotted in the figure. In both cases, we found that DTS values almost linearly increased with the molding pressure. Dependence of the DTS on molding pressure was much larger in the compact after carbonation, as shown in larger slope of the regression line. Thus the extent of increase in DTS by the carbonation became larger with the molding pressure.

Discussion

The results obtained in the present study clearly demonstrated that $Ca(OH)_2$ transformed directly to calcite, which is a most stable phase of calcium carbonate [11] when calcium hydroxide compacts were carbonated in CO_2 gas saturated with water vapor. The carbonation rate was almost the same irrespective of molding pressure and the carbonation almost completed within 72 h. At higher molding pressure, however, a small diffraction peak of $Ca(OH)_2$ was still found at 2θ of 34.1° even after 72 h. Final conversion rate decreased from 99.8 wt% to 86.3 wt% with increasing in the molding pressure. This is probably caused by less penetration of CO_2 gas through

interparticles due to dense packing at higher molding pressure. In the other words, the $Ca(OH)_2$ compact prepared at higher molding pressure had less porosity, as shown in Fig. 3.

We also found that diffraction peaks of the calcite formed were broader than a commercially available calcite powder, which is well crystallized. Since the broadening of the diffraction peak is usually seen when the crystallite size became smaller, it is reasonable to consider that crystallite size of the calcite formed by the carbonation was smaller than the commercial one. As shown in Table 2, the crystallite size of the calcite obtained was between 35.2 nm and 46.8 nm and much smaller than that (83.4 nm) of the commercial calcite. The small crystallite size is preferable when the material is used as a bone substitute or a precursor of carbonate apatite preparation as a biomaterial.

During carbonation, no morphological changes was observed even at SEM level, it is probably due to the small crystallite size of calcite formed as already described. Therefore fine calcite crystals developed on the $Ca(OH)_2$ particles with keeping its original shape. As a matter of fact, the porosity was slightly decreased by about 4% before and after carbonation at each molding pressure. The decrease in porosity almost corresponds to a theoretical decrease of about 6% calculated under an assumption that a certain amount of $Ca(OH)_2$ compact transforms into calcite without changing its original volume. The carbonation proceeded by diffusion of CO_2 gas through the calcite layer initially formed on the original $Ca(OH)_2$ particle. Basically, smaller and less pores were observed in the $Ca(OH)_2$ compact prepared at higher molding pressure. This is also clearly demonstrated by change in porosity of $Ca(OH)_2$ compact after carbonation for 72 h with various molding pressure as shown in Fig. 3.

DTS rapidly increased in a first few hours and after that it gradually increased as shown in Fig. 4. The initial rapid increase is caused by the interparticle binding through calcite formed on the surface of the original $Ca(OH)_2$ particles. As already described, the extent of increase in DTS by the carbonation was larger at higher molding pressure, which was more effective for an intimate contact among the particles resulting in tight interparticle binding. As seen in Figs. 3 and 5, porosity decreases with molding pressure. This fact suggests that the final DTS mainly depends on the porosity. Actually, the following equation was theoretically derived to explain the relationship between the mechanical strength and porosity in brittle solid such as gypsum [12, 13]:

$$S = S_0 \log(P_{Cr}/P),$$

where S denotes mechanical strength and P denotes porosity. S_0 is a constant and P_{Cr} is defined as a critical

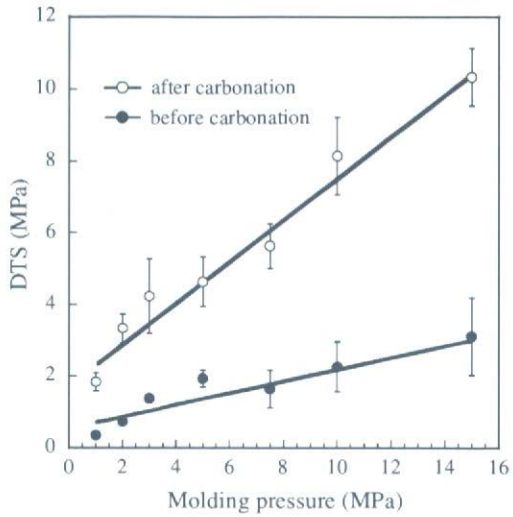

Fig. 5 DTS values before and after carbonation for 72 h plotted against molding pressure. The bars in the figure denote standard deviation

porosity, where the strength S becomes zero. Later, the equation was applied for the mechanical strength of dental gypsum [14] and biological calcium phosphate cement [15]. Figure 6 shows the relationship between DTS values and logarithm of porosity of specimens prepared at various molding pressures and those carbonated for 72 h. It was found that DTS values are inversely proportional to logarithm of porosity, that is, the above equation well holds. Critical porosity, P_{Cr} can be obtained by the extrapolation of the regression lines to zero of DTS. With the compact before and after the carbonation, P_{Cr} was 64.6% and

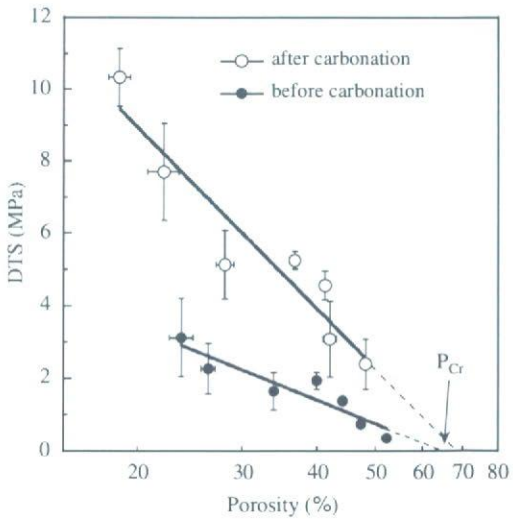

Fig. 6 The relation between DTS and logarithm of porosity of $Ca(OH)_2$ compacts before and after carbonation for 72 h. The bars in the figure denote standard deviation

68.4%, respectively, and both values almost coincided. This fact suggested that DTS values are determined by porosity in the calcite compact.

As shown in Fig. 5, specimens after carbonation for 72 h followed by being pressed at 1 MPa showed DTS values of 1.84 ± 0.25 MPa, and then linearly increased with the molding pressure, finally attained to 10.33 ± 0.80 MPa in the case of being pressed at 15 MPa, which is similar to that of set gypsum. The mechanical strengths are not sufficient for application to the areas exposed to large stress such as discontinuity defects of the jaw bones. However, it is enough for non load bearing area such as the holey bone defects caused by extirpation of tumors and cysts and the alveolar bone defects resulting from periodontal diseases. Moreover, when the calcite block is used as a bone substitute or as a precursor for the apatite like a coralline apatite, macroporosity plays an important role for penetration of cells and tissue fluid. Trial for fabrication of macroporus calcite block with higher porosity is now progress in our laboratory and a part of study will be published elsewhere [16].

Conclusion

For an artificial bone substitute, we prepared calcite compacts by carbonation of $Ca(OH)_2$ compacts under various molding pressures ranged from 1 MPa to 15 MPa in CO_2 gas saturated with water vapor for various periods up to 72 h. It was found that $Ca(OH)_2$ transformed directly to calcite and the transformation was not completed at higher molding pressure though its rate was almost the same irrespective of molding pressure. It was also found that DTS were determined by porosity in the calcite compact depending on molding pressure. There was a linear relation between DTS and logarithm of porosity.

This method enables us to obtain calcium carbonate compact with a wide range of mechanical strength by controlling the molding pressure.

Acknowledgments This study was supported in part by a Grant-in-aid for Scientific Research from the Ministry of Education, Sports, Culture, Science, and Technology, Japan.

References

1. F. SOUYRIS, C. PELLEQUER, C. PAYROT and C. SERVERA, *J. Maxillofac. Surg.* **13**(2) (1985) 64
2. G. GUILLEMIN, J. L. PATAT, J. FOURNIE and M. CHETAIL, *J. Biomed. Mater. Res.* **21**(5) (1987) 557
3. J. L. PATAT and G. GUILLEMIN, *Annal Chirurg Plast Esthet* **34**(3) (1989) 221
4. F. X. ROUX, D. BRASNU, B. LOTY, B. GEORGE and G. GUILLEMIN, *J. Neurosurg.* **69**(4) (1988) 510
5. F. X. ROUX, B. LOTY, D. BRASNU and G. GUILLEMIN, *Neuro-Chirurgie* **34**(2) (1988) 110
6. D. M. ROY and S. K. LINNEHAN, *Nature* **247** (1974) 220
7. M. SIVAKUMAR, T. S. KUMAR, K. L. SHANTHA and K. P. RAO, *Biomaterials* **17** (1996) 1709
8. W. SUCHANEK and M. YOSHIMURA, *J. Mater. Res.* **13** (1998) 94
9. J. C. FRICAIN, R. BAREILLE, F. ULYSSE, B. DUPUY and J. AMDEE, *J. Biomed. Mater. Res.* **42** (1998) 96
10. S. MATSUYA, X. LIN, K. UDOH, M. NAKAGAWA, R. SHIMOGORYO, Y. TERADA and K. ISHIKAWA, *J. Mater. Sci.: Mater. Med.* (2006) in press
11. L. N. PLUMMER and E. BUSENBERG, *Geochim Cosmochim Acta* **46** (1982) 1011
12. K. K. SCHILLER, in "Mechanical properties of non metallic brittle solids", edited by W. H. Walton (Butterworth, London, 1958) p. 35
13. K. K. SHIHILLER, *Br. J. Appl. Phys.* **11** (1960) 338
14. T. MORI and M. YAMANE, *Aust. Dent. J.* **27**(1) (1982) 30
15. K. ISHIKAWA and K. ASAOKA, *J. Biomed. Mater. Res.* **29**(12) (1995) 1537
16. Y. LEE, Y. M. HAHM, S. MATSUYA, M. NAKAGAWA and K. ISHIKAWA, *J. Mater. Sci.* (2006) in press

Mater. Res. Soc. Symp. Proc. Vol. 971 © 2007 Materials Research Society 0971-Z07-12

Development of Environmental Cell and its Application to Hydrogen Storage Materials

Koya Okudera[1], Koichi Hamada[1], Takanori Suda[1], Naoyuki Hashimoto[1], Somei Ohnuki[1], Yasuaki Kawai[2], and Yoshitsugu Kojima[3]

[1]Division of Materials Science and Engineering, Graduate School of Engineering, Hokkaido University, Sapporo, Hokkaido, 060-8628, Japan

[2]Toyota Central R&D Labs. Inc., Nagakute, Aichi, 480-1192, Japan

[3]Institute for Advanced Materials Research, Hiroshima University, Higashi-Hiroshima, Hiroshima, 739-8530, Japan

ABSTRACT

"Environmental cell" microscopy was applied for surveying the reaction of hydrides in vanadium and magnesium based alloys, which are candidates for hydrogen storage materials of advanced hydrogen energy systems. In order to clarify the mechanism of hydrogenation process, *in-situ* experiment was carried out by using a 200 kV transmission electron microscope (TEM) equipped with a newly developed environmental cell (EC), which is capable to investigate transmitted image and electron-diffraction under gas hydrogen environment of 0.1 MPa at room temperature. In case of vanadium, under hydrogen-gas of 0.1 MPa, bending fringe was created probably due to local stress induced with the hydrogen solution. On the other hand, when hydrogen gas reacted with magnesium powders, swelling due to volume expansion was occurred. In practice, surface steps with several ten nm became straightened, and additionally, the formation of MgH_2 was indicated in selected-area diffraction pattern (SADP). *In-situ* experiment for hydrogenation reaction by using the environmental cell was recently started. The precise studies, as well as its improvement, will be continued, especially in the transparence films.

INTRODUCTION

The hydrogen storage alloy attracts attention as one of the hydrogen storage materials. Although many studies have been done for development of better materials, microscopic observation of the hydrogen absorption reaction process aiming at evaluation or control of material has not been performed. TEM observation and *in-situ* XRD analysis are carried out to understand effects of microstructures and temporal structure changes. (e.g. reference [1],[2]). Although these ways are very effective for understanding of material properties, it isn't able to observe successive microstructural changes with hydrogenation. We thought the environmental cell enables to observe them and it is useful to the development of advanced hydrogen storage materials.

Environmental cell is a technique for *in-situ* observation in TEM. In the past study, *in-situ* observation of the oxidation process of Ni-Cr alloy was performed using the HVEM which is the acceleration voltage of 1.2 MV (pressure 2.4-2.8 kPa, temperature of 500 °C) [3]. In the catalytic reaction, P. L. Gai *et al.* are performing *in-situ* observation for the catalytic reaction of molybdic acid bismuth which is a heterogeneous catalyst on 100 Torr and 400-500 °C conditions using C_3H_6 gas [4]. As an example of the *in-situ* observation of crystal growth, cryostat is

introduced in a microscope and *in-situ* observation of crystal growth process of sulfur hexafluoride (SF_6) is performed at 50 Torr and below 150 K [5]. As the multiple usages with open-type environmental cell other than heating, there is a case which is doing the tensile test pouring hydrogen gas, and the interaction of hydrogen and a rearrangement is observed [6].

Although the above cases of application of environmental cells were reported, the environmental cell had not been used for the hydrogen storage alloys. In this study, therefore, an environmental cell capable to build gas environment in a column without converting a TEM body was manufactured in order to perform *in-situ* observation of a hydrogen absorption reaction. As the first report of *in-situ* observation of the hydrogenation reaction process, vanadium and magnesium were investigated using the manufactured environmental cell.

EXPERIMENTAL

The scheme of the newly manufactured environmental cell

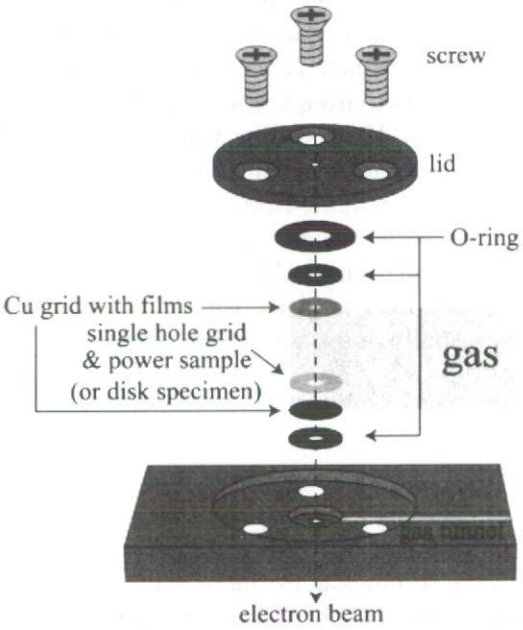

Figure 1. The schematic view of the nose of environmental cell holder

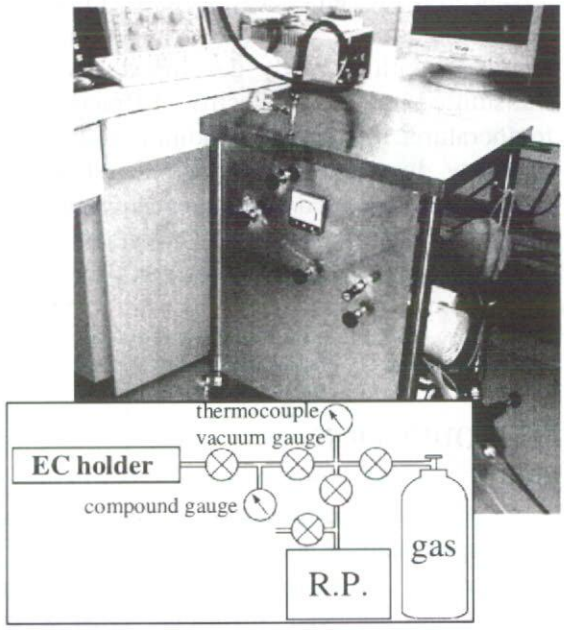

Figure 2. Photograph of the gas-control part and schematic view of a gas-control system

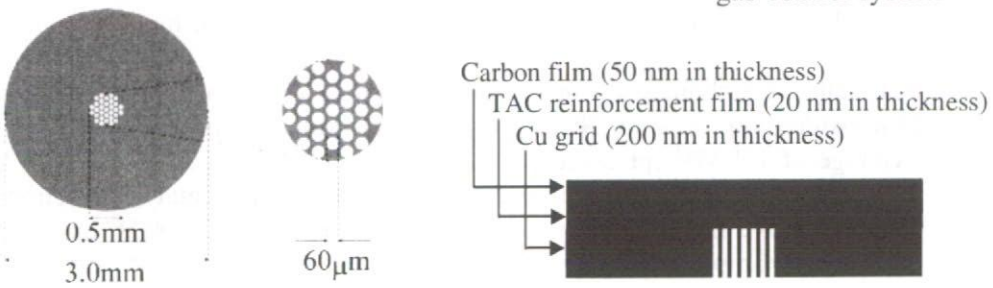

Figure 3. The schematic view of an electron-transparent grid

The holder manufactured was a modified holder of a general-purpose type TEM (JEOL JEM-2010). The environmental cell holder is mainly made of aluminum, and the acroteric is brass. The stainless steel pipe with a valve, which is for the path of gas, is located in the inside of this holder. The schematic view of the nose of a holder is shown in figure 1. This environmental cell is a closed (window) type and airtightness is kept by three O-rings about 0.2 mm in thick and the grid of two upper and lower sides by which the film was covered. The narrow tunnel is extended toward the acroteric hollow and gas flows through this. Moreover, this narrow tunnel is connected with the stainless steel pipe in a holder. Figure 2 is a photograph of a gas-control part of an environmental cell, and a schematic view of a gas-control system. The tube extended from the inside of a holder is connected with the gas-control part which has a rotary pump and a gas cylinder. By this gas-control part, arbitrary gas can be introduced from several pascals to 0.1 MPa. Figure 3 is a schematic view of a grid. The grid is made of copper with the carbon film (50 nm in thick), which is stabilized with the triacetyl cellulose (TAC) film (20 nm in thick). The TAC is stable against accelerated electron beam [7], so that observation can be carried out without breaking vacuum in column. A single hole grid is used as a spacer when using a powder sample.

Sample preparation

The powder of magnesium hydride (MgH_2, Alfa Aesar) packed into the quartz tube with a valve was heat-treated at about 250 °C for 1 hour in electric furnace with a diffusion pump for degassing. This dehydrogenated Mg powder was used as a Mg sample.

Pure vanadium used in this study was provided from National Institute for Fusion Science (NIFS). The vanadium was cold-rolled to 0.1 mm in thick. Subsequently, a TEM disc (3 mm in diameter) was punched out, followed by the vacuum encapsulation with the zirconium foil as oxygen getter at the quartz tube. The quartz tube was annealed in an electric furnace at 900 °C for 30 minutes, and air-cooled. The TEM disc was electro-polished using a twin jet electrolytic-polishing device (TenuPol-5), at 9 V and 20 °C with a solution of sulfuric (80 %) and methanol (20 %). The electro-polished sample was immediately put into ethanol in order to avoid oxidation of surface, and dried within a glove box.

Specimen loading to the environmental cell

Primarily, the head of the environmental cell holder was cleaned by ethanol with ultrasonic. In order to remove the ethanol, which might adhere into a holder line, bake-out was carried out with a pre-evacuation device at 55 °C for 1 hour. For preventing oxidation and keeping surface activity, the holder was loaded with the sample within the globe box in argon atmosphere. Firstly, O-ring, Cu grid, two sheets of single hole grid and paper lid are attached to the head of a holder in the air. The edge of upper single hole grid is folded so that it may be easy to remove. This single hole grid is for making powder covers only the center of grid. Then, the valve of the environmental cell holder was opened, so that it might be easy to flow through gas. After these steps were completed, a stereoscopic microscope, an environmental cell holder, a sample and tools were put in the glove box. A stereoscopic microscope is used for precise specimen setting. The inside of a glove box is evacuated using a rotary pump, and it is filled up with the argon gas at an atmospheric pressure. This process has done twice. And the following processes were carried out within a glove box.

When Mg powder was picked with tweezers and dropped on the grid, the holder was set upside-down struck it lightly, and then, big powders that might break films were dropped. Small powder only remained on the film of a grid by this process. After carrying a sample, the paper lid and the folded single hole grid tend to be dismounted, so that the lid with two O-rings was stabilized with screws. In the case of vanadium, the single hole grid is not necessary. The TEM disc was set instead of it. Finally, the valve of the environmental cell holder was closed and it took out from the glove box.

The holder loaded with the sample was inserted in TEM (JEOL JEM-2010). In observation of magnesium, bright filed images and selected-area-diffraction patterns were taken before hydrogen introduction. The argon gas in an environmental cell holder was evacuated with the rotary pump after photographing. Subsequently, H_2 gas of 0.1 MPa was introduced, and some images were taken in the same manner. When vanadium sample was observed, images were taken using DigitalVideo by a CCD camera.

RESULT AND DISCUSSION

In-situ observation of the hydrogenation of V

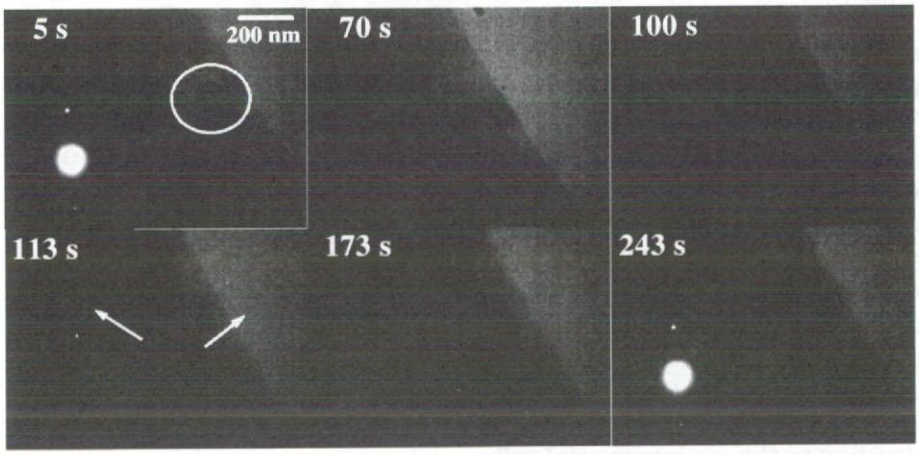

Figure 4. Sequence BF image and SADP of vanadium after the hydrogen introduction

Figure 4 shows sequence image of the hydrogenation reaction of vanadium. These images were recorded by DigitalVideo. As shown in figure 4, distortion seemed to be occurred locally and the interference fringe (black contrast) was observed. In addition, spreading and moving of interference fringe were observed, suggesting that a strain was locally produced when hydrogen solid-solve to vanadium and moving continuously. This interference fringe actually moved for about 20 minutes On the other hand, this remarkable change was not seen in diffraction pattern, meaning that there is no formation of hydride. The plateau area for a low pressure area of vanadium is 1 Pa or less, and the gas pressure of the hydrogen introduced this time is 0.1 MPa. Even if there are some leaks, the hydride of vanadium (V_2H) should be generated theoretically. This result suggested that the surface condition of vanadium would be a key. The oxide film or hydroxide (it originates in electrolytic polishing) could be formed on the specimen surface. Basically, vanadium is a metal which chemical attraction with oxygen is very

strong and initial activity is bad [8]. In order to observe the formation reaction of hydride using the environmental cell manufactured this time, a contamination-free specimen should be required.

In-situ observation of the hydrogenation of Mg

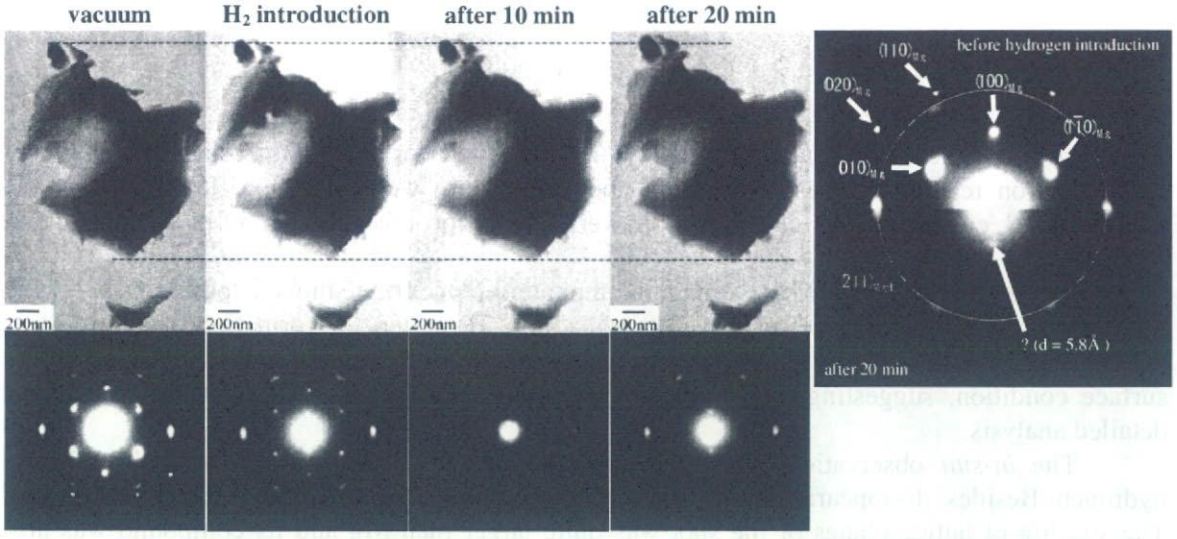

Figure 5. BF and SADP of Mg particles before and after introducing hydrogen.

Figure 5 shows the bright field (BF) images and selected-area-diffraction patterns (SADP) of Mg grains before and after hydrogen introduction. The broken line shows the grain size before hydrogen introduction. As shown in a figure 5, grains were expanded slightly after introducing hydrogen. In the photograph before hydrogen introduction and after introduction for 20 minutes, maximum width of grains was increased about 10 % and the cross-sectional area seemed to be increased about 28 %.

Moreover, it assumed that the measured cross-sectional area was equivalent to the cross-sectional area of a sphere, and the rate of volume increase was calculated. It seems that the volume of the grains hydrogen-introduced for 20 minutes increased about 40 %. From the crystal structure and the lattice constant of Mg and MgH_2, it is expected that the ideal cubical expansion by hydrogenation is about 30 %, suggesting that the assumption used this time for the estimation of volume expansion was not appropriate.

A right viewgraph in figure 5 is the comparison of SADP before and after introduction for 20 minutes. The spacing of lattice planes corresponding to a spot is calculated from the following formula: ($d = \lambda L/R$).

Where λ is wavelength of electron beam (=0.0251 Å at 200 kV), L is camera length (=80 cm) and R is the distance between a spot and center. With R measured from the film, the spacing of lattice planes, d, can be calculated. Furthermore, the value of the spacing of lattice planes, d, and the calculated value from JCPDS card (Mg, Mg oxides, and MgH_2) were compared, and also Miller indices were determined. There is a spot disappeared in 20 minutes after hydrogen introduction. It is probably a pattern from Mg because the Mg sample used this time was simple substance. Moreover, there is a firm ring-like pattern before and after hydrogen introduction, and this is considered to be a pattern from MgH_2. There is a possibility that the dehydrogenation of MgH_2

was incomplete. Although dehydrogenation was carried out at 250 °C, unless MgH_2 might be heated up to 600 K, dehydrogenation does not fully occur. Therefore, it is almost certain that MgH_2 exists at the time before the hydrogen introduction in this experiment.

Although diffraction spots showing d=5.8 Å were observed in this experiment, we could not identify what they resulted from.

SUMMARY

Using the environmental cell newly manufactured for the *in-situ* observation of the hydrogenation reaction process, vanadium and magnesium were observed. It seems that the manufactured environmental cell was a powerful tool for investigation of a hydrogenation reaction.

In the *in-situ* observation of vanadium, the interference fringe moved continuously for the local distortion by hydrogen solid-solved to vanadium. However, the formation of hydride was not observed. Observation of hydrogenation reaction in vanadium tends to be influenced by the surface condition, suggesting that contamination-free surface specimen would be needed for detailed analysis.

The *in-situ* observation of magnesium indicated grain expansion due to introducing hydrogen. Besides, disappearing of diffraction spot during hydrogenation reaction was observed. The spacing of lattice planes of the spot was quite larger than Mg and its compound was also seen, however, what it is a pattern resulting from had unknown.

ACKNOWLEDGMENTS

In this study, the accumulation of technical know-how of experiments by seniors was very beneficial. Author would like to take this opportunity to thank to K. Takase and K. Yashiki who are graduated students of Hokkaido University.

REFERENCES

1. T. Yamamoto, H. Inui and M. Yamaguchi, Mater. Sci. Eng. A, **329-331** 367-371 (2002)
2. T. Nakagawa, T. Ichikawa, R. Iida, H. Leng, N. Takeichi, T. Kiyobayashi, H. Takeshita and H. Fujii, J. Alloys Comp., **430** 217-221 (2007)
3. P. Marikar, M. B. Brodsky, C. H. Sowers, N. J. Zaluzec, Ultramicroscopy, **29** 247-256 (1989)
4. P. L. Gai, J. Solid State Chem., **49** 25-42 (1983)
5. G. Raynerd, J. A. Venables, **23** 432-433 (1987)
6. I. M. Robertson, Engineering Fracture Mechanics, **68** 671-692 (2001)
7. T. Akimoto, Y. Hirohata, M. Shimada, H. Sugi, Proceedings of the 57th Annual Meeting of the Japanese Society of Electron Microscopy, 119 (2001)
8. K. Fujita, Y. C. Huang, M. Tada, J. Japan Inst. Metals, **43** 601-609 (1979)

Advanced Materials Research Vols. 26-28 (2007) pp. 877-880
online at http://www.scientific.net

Online available since 2007/10/02

Development of Environmental Cell for Gas Reaction of Nano-size Particles

Koya Okudera[1, a], Koichi Hamada[1,b], Takanori Suda[1,c], Naoyuki Hashimoto[1,d], Somei Ohnuki[1,e]

[1]Division of Materials Science and Engineering, Graduate School of Engineering, Hokkaido University, Sapporo, Hokkaido, 060-8628, Japan

[a]okudera@eng.hokudai.ac.jp, [b]hamada@nano.ist.hokudai.ac.jp, [c]suda@eng.hokudai.ac.jp, [d]hasimoto@eng.hokudai.ac.jp, [e]ohnuki@eng.hokudai.ac.jp

Keywords: in-situ, TEM, environmental cell, hydrogen storage alloy, magnesium

Abstract. "Environmental cell" microscopy was applied for surveying gas reaction of hydrides in magnesium base alloys, which are candidates for hydrogen storage materials in advanced hydrogen energy systems. In order to clarify the mechanism of hydrogenation process, in-situ experiment has been carried out by using a 200 kV transmission electron microscope (TEM) equipped with a newly developed environmental cell, which is capable to 0.1 MPa in the temperature range between R.T. and 200°C. When hydrogen gas reacted with magnesium powders, straightening of surface steps (60~70 nm in height) was observed, indicating that volume expansion occurred. In addition, the formation of MgH2 was indicated in selected-area-diffraction patterns (SADP). The precise study on this in-situ experiment, as well as its improvement, will be continued, with using transparent films.

Introduction

The hydrogen storage alloy attracts attention as one of the hydrogen storage materials. Although many studies have been done for development of better materials, microscopic observation of the hydrogen absorption reaction process aiming at evaluation or control of material has not been performed. TEM observation and *in-situ* XRD analysis are carried out to understand effects of microstructures and temporal structure changes. (e.g. reference [1],[2]). Although these ways are very effective for understanding of material properties, it isn't able to observe successive microstructural changes with hydrogenation. We thought the environmental cell enables to observe them and it is useful to the development of advanced hydrogen storage materials.

Environmental cell is a technique for *in-situ* observation in TEM. In the past study, *in-situ* observation of the oxidation process of Ni-Cr alloy was performed using the HVEM which is the acceleration voltage of 1.2 MV (2.4-2.8 kPa, 500 °C) [3]. In the catalytic reaction, P. L. Gai *et al.* are performing *in-situ* observation for the catalytic reaction of molybdic acid bismuth which is a heterogeneous catalyst on 100 Torr and 400-500 °C conditions using C_3H_6 gas [4]. As an example of the *in-situ* observation of crystal growth, cryostat is introduced in a microscope and *in-situ* observation of crystal growth process of sulfur hexafluoride (SF_6) is performed at 50 Torr and below 150 K [5]. As the multiple usages with open-type environmental cell other than heating, there is a case which is doing the tensile test pouring hydrogen gas, and the interaction of hydrogen and a rearrangement is observed [6].

Although the above cases of application of environmental cells were reported, the environmental cell had not been used for the hydrogen storage alloys. In this study, therefore, an environmental cell capable to build gas environment in a column without converting a TEM body was manufactured in order to perform *in-situ* observation of a hydrogen absorption reaction. As the first report of *in-situ* observation of the hydrogenation reaction process, magnesium was investigated using the manufactured environmental cell.

Experimental

The scheme of the newly manufactured environmental cell. The holder manufactured was a modified holder of a general-purpose type TEM (JEOL JEM-2010). The environmental cell holder is mainly made of aluminum, and the acroteric is brass. The stainless steel pipe with a valve, which is for the path of gas, is located in the inside of this holder. The schematic view of the nose of a holder is shown in figure 1. This environmental cell is a closed (window) type and airtightness is kept by three O-rings about 0.2 mm in thick and the grid of two upper and lower sides by which the film was covered. The narrow tunnel is extended toward the acroteric hollow and gas flows through this. Moreover, this narrow tunnel is connected with the stainless steel pipe in a holder. Figure 2 is a photograph of a gas-control part of an environmental cell, and a schematic view of a gas-control system. The tube extended from the inside of a holder is connected with the gas-control part which has a rotary pump and a gas cylinder. By this gas-control part, arbitrary gas can be introduced from several pascals to 0.1 MPa. Figure 3 is a schematic view of a grid. The grid is made of copper with the carbon film (50 nm in thick), which is stabilized with the triacetyl cellulose (TAC) film (20 nm in thick). The TAC is stable against accelerated electron beam [7], so that observation can be carried out without breaking vacuum in column. A single hole grid is used as a spacer when using a powder sample.

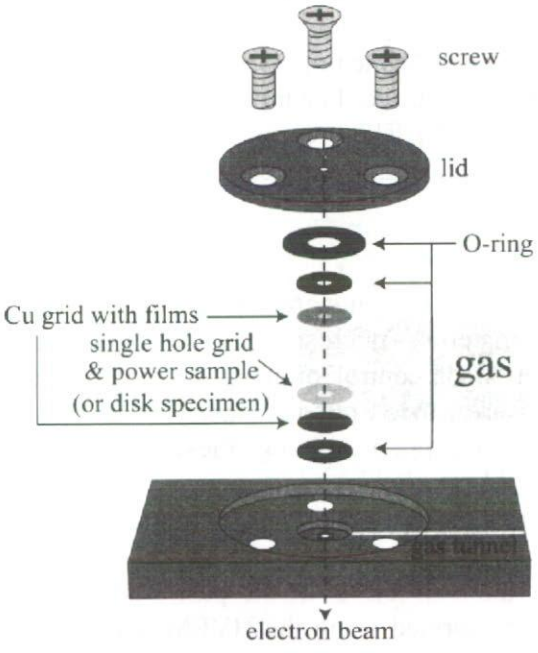

Figure 1. The schematic view of the nose of environmental cell holder

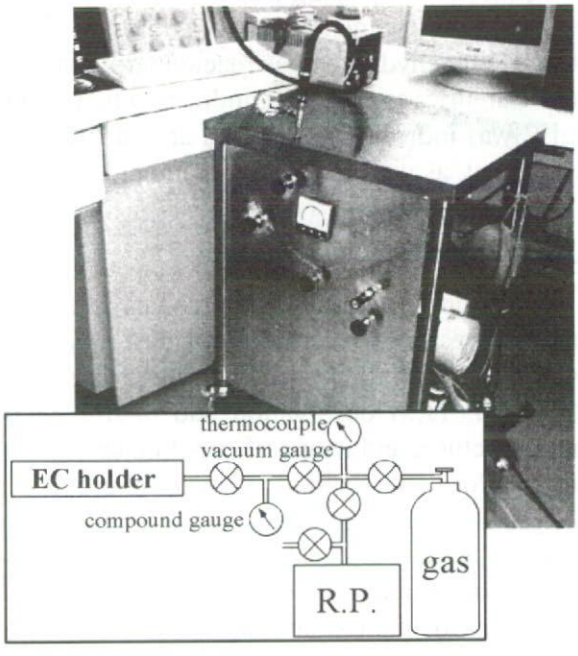

Figure 2. Photograph of the gas-control part and schematic view of a gas-control system

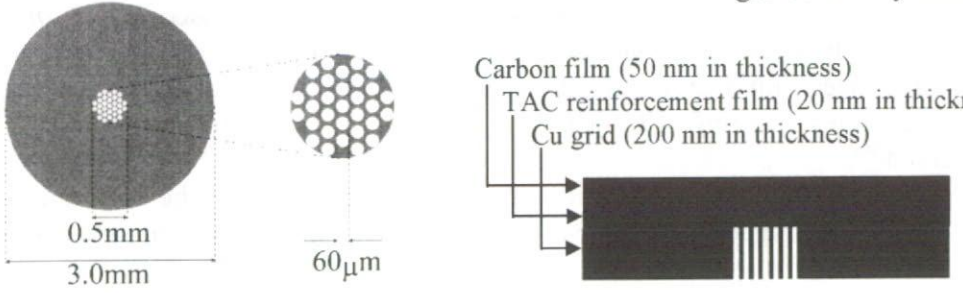

Figure 3. The schematic view of an electron-transparent grid

Sample preparation and loading. The powder of magnesium hydride (MgH_2, Alfa Aesar) packed into the quartz tube with a valve was heat-treated at about 250 °C for 1 hour in electric furnace with a diffusion pump for degassing. This dehydrogenated Mg powder was used as a Mg sample.

Primarily, the head of the environmental cell holder was cleaned by ethanol with ultrasonic. In order to remove the ethanol, which might adhere into a holder line, bake-out was carried out with a pre-evacuation device at 55 °C for 1 hour. For preventing oxidation and keeping surface activity, the holder was loaded with the sample within the globe box in argon atmosphere. Firstly, O-ring, Cu grid, two sheets of single hole grid and paper lid are attached to the head of a holder in the air. The edge of upper single hole grid is folded so that it may be easy to remove. This single hole grid is for making powder covers only the center of grid. Then, the valve of the environmental cell holder was opened, so that it might be easy to flow through gas. After these steps were completed, a stereoscopic microscope, an environmental cell holder, a sample and tools were put in the glove box. A stereoscopic microscope is used for precise specimen setting. The inside of a glove box is evacuated using a rotary pump, and it is filled up with the argon gas at an atmospheric pressure. This process has done twice. And the following processes were carried out within a glove box.

When Mg powder was picked with tweezers and dropped on the grid, the holder was set upside-down struck it lightly, and then, big powders that might break films were dropped. Small powder only remained on the film of a grid by this process. After carrying a sample, the paper lid and the folded single hole grid tend to be dismounted, so that the lid with two O-rings was stabilized with screws. The TEM disc was set instead of it. Finally, the valve of the environmental cell holder was closed and it took out from the glove box.

The holder loaded with the sample was inserted in TEM (JEOL JEM-2010). In observation of magnesium, bright filed images and selected-area-diffraction patterns were taken before hydrogen introduction. The argon gas in an environmental cell holder was evacuated with the rotary pump after photographing. Subsequently, H_2 gas of 0.1 MPa was introduced, and some images were taken in the same manner.

Result and discussion

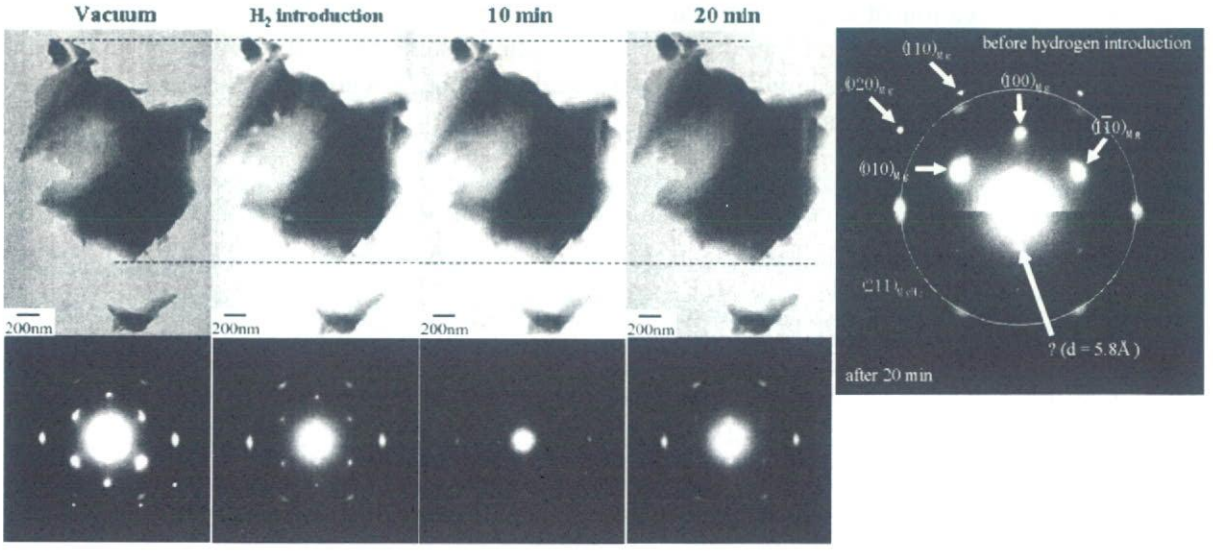

Figure 4. BF and SADP of Mg particles before and after introducing hydrogen.

Figure 4 shows the bright field (BF) images and SADP of Mg grains before and after hydrogen introduction. The broken line shows the grain size before hydrogen introduction. As shown in a figure 4, grains were expanded slightly after introducing hydrogen. In the photograph before hydrogen

introduction and after introduction for 20 minutes, maximum width of grains was increased about 10 % and the cross-sectional area seemed to be increased about 28 %.

Moreover, it assumed that the measured cross-sectional area was equivalent to the cross-sectional area of a sphere, and the rate of volume increase was calculated. It seems that the volume of the grains hydrogen-introduced for 20 minutes increased about 40 %. From the crystal structure and the lattice constant of Mg and MgH_2, it is expected that the ideal cubical expansion by hydrogenation is about 30 %, suggesting that the assumption used this time for the estimation of volume expansion was not appropriate.

A right viewgraph in figure 5 is the comparison of SADP before and after introduction for 20 minutes. The spacing of lattice planes corresponding to a spot is calculated from the following formula: ($d = \lambda L/R$). Where λ is wavelength of electron beam (=0.0251 Å at 200 kV), L is camera length (=80 cm) and R is the distance between a spot and center. With R measured from the film, the spacing of lattice planes, d, can be calculated. Furthermore, the value of the spacing of lattice planes, d, and the calculated value from JCPDS card (Mg, Mg oxides, and MgH_2) were compared, and also Miller indices were determined. There is a spot disappeared in 20 minutes after hydrogen introduction. It is probably a pattern from Mg because the Mg sample used this time was simple substance. Moreover, there is a firm ring-like pattern before and after hydrogen introduction, and this is considered to be a pattern from MgH_2. There is a possibility that the dehydrogenation of MgH_2 was incomplete. Although dehydrogenation was carried out at 250 °C, unless MgH_2 might be heated up to 600 K, dehydrogenation does not fully occur. Therefore, it is almost certain that MgH_2 exists at the time before the hydrogen introduction in this experiment.

Although diffraction spots showing d=5.8 Å were observed in this experiment, we could not identify what they resulted from.

Summary

Using the environmental cell newly manufactured for the *in-situ* observation of the hydrogenation reaction process, magnesium was observed. It seems that the manufactured environmental cell was a powerful tool for investigation of a hydrogenation reaction.

The *in-situ* observation of magnesium indicated grain expansion due to introducing hydrogen. Besides, disappearing of diffraction spot during hydrogenation reaction was observed. The spacing of lattice planes of the spot was quite larger than Mg and its compound was also seen, however, what it is a pattern resulting from had unknown.

References

[1] T. Yamamoto, H. Inui and M. Yamaguchi: Mater. Sci. Eng. A, 329-331 367-371 (2002)
[2] T. Nakagawa, T. Ichikawa, R. Iida, H. Leng, N. Takeichi, T. Kiyobayashi, H. Takeshita and H. Fujii: J. Alloys Comp., 430 217-221 (2007)
[3] P. Marikar, M. B. Brodsky, C. H. Sowers and N. J. Zaluzec: Ultramicroscopy, 29 247-256 (1989)
[4] P. L. Gai, J. Solid State Chem., 49 25-42 (1983)
[5] G. Raynerd, J. A. Venables, 23 432-433 (1987)
[6] I. M. Robertson: Engineering Fracture Mechanics, 68 671-692 (2001)
[7] T. Akimoto, Y. Hirohata, M. Shimada and H. Sugi: Proceedings of the 57th Annual Meeting of the Japanese Society of Electron Microscopy, 119 (2001)

厚生労働科学研究費補助金

化学物質リスク研究事業

ナノ微粒子の体内動態可視化法の開発

（課題番号 ： H18-化学--一般-006）

平成１９年度秋期
第３回研究成果発表会

日時：平成 19 年 11 月 12 日～13 日

場所：登別市「第一滝本館」

平成19年度研究組織

［主任研究者］

亘理 文夫	北海道大学大学院歯学研究科　口腔健康科学講座　教授

［分担研究者］

田路 和幸	東北大学大学院環境科学研究科　教授
戸塚 靖則	北海道大学大学院歯学研究科　口腔病態学講座　教授
横山 敦朗	北海道大学大学院歯学研究科　口腔機能学講座　教授
北川 善政	北海道大学大学院歯学研究科　口腔病態学講座　教授
森田　学	北海道大学大学院歯学研究科　口腔健康科学講座　教授
朝倉 清高	北海道大学触媒科学研究センター　教授
古月 文志	北海道大学大学院地球環境科学院　教授
大貫 惣明	北海道大学大学院工学研究科　教授
遠山 晴一	北海道大学大学院医学研究科　准教授
石川 邦夫	九州大学大学院歯学研究科　教授
岡崎 正之	広島大学大学院医歯薬学総合研究科　教授
浅岡 憲三	徳島大学ヘルスバイオサイエンス研究部　教授

［研究協力者（順不同）］

大森 守	東北大学　エネルギー安全科学国際研究センター　研究支援者
橋田 俊之	東北大大学大学院工学研究科 教授
矢田 慶治	東北大学　名誉教授
奥山 文雄	名古屋工業大学　名誉教授
久保木 芳徳	北海道大学　名誉教授
芳賀 信幸	石巻専修大学大学院理工学研究科　教授
水野 峰男	（財）ファインセラミックスセンター　主席研究員
橋本 雅美	（財）ファインセラミックスセンター　副主任研究員
市野瀬 英喜	（独）理化学研究所
竹内 あかり	九州大学大学院歯学研究科　助教
植野 哲	徳島大学ヘルスバイオサイエンス研究部　准教授
米澤 徹	東京大学 大学院理学系研究科　准教授
林 靖彦	名古屋工業大学都市循環システム工学専攻　助教
佐藤 義倫	東北大学大学院環境科学研究科　助教
韮澤 崇	ブルカー・ダルトニクス株式会社
田中 信夫	名古屋大学大学院工学研究科　教授
坂口 紀史	北海道大学エネルギー変換マテリアル研究センター　准教授
小野寺 伸	北海道大学大学院医学研究科　運動機能再建医学分野　助教
川浪 雅光	北海道大学大学院歯学研究科　口腔健康科学講座　教授

菅谷　勉　　北海道大学大学院歯学研究科　口腔健康科学講座　准教授
八若 保孝　　北海道大学大学院歯学研究科　口腔機能学講座　教授
加我 正行　　北海道大学大学院歯学研究科　口腔機能学講座　准教授
宇尾 基弘　　北海道大学大学院歯学研究科　口腔健康科学講座　准教授
赤坂 司　　北海道大学大学院歯学研究科　口腔健康科学講座　助教
阿部薫明　　北海道大学大学院歯学研究科　口腔健康科学講座　助教
高師 則行　　北海道大学大学院歯学研究科　口腔病態学講座　助教
野田坂佳伸　　北海道大学大学院歯学研究科　中央研究部　助教
天雲 太一　　北海道大学大学院歯学研究科　口腔健康科学講座　歯科医師
朱 禹赫　　北海道大学大学院歯学研究科　口腔健康科学講座　専門研究員
Xiaoming Li　北海道大学大学院歯学研究科　口腔健康科学講座　外国人特別研究員
阿部 大基　　石巻専修大学大学院理工学研究科　大学院生
寺田 典子　　北海道大学大学院歯学研究科　口腔病態学講座　大学院生
石川 紘佑　　北海道大学大学院歯学研究科　口腔機能学講座　大学院生
伊藤 佐智子　北海道大学大学院歯学研究科　口腔機能学講座　大学院生
松岡 真琴　　北海道大学大学院歯学研究科　口腔病態学講座　大学院生
平田 恵理　　北海道大学大学院歯学研究科　口腔機能学講座　大学院生
江崎 光恵　　北海道大学大学院歯学研究科　口腔健康科学講座　大学院生
林 春　　北海道大学　大学院地球環境科学研究院　大学院生
藤井 明洋　　北海道大学　大学院地球環境科学研究院　大学院生
譚 暁明　　北海道大学　大学院地球環境科学研究院　大学院生

厚生労働科学研究費補助金　化学物質リスク研究事業
「ナノ微粒子体内動態可視化法の開発」　(H18-化学--一般-006)

第３回研究成果発表会プログラム

１１月１２日（月）

１３：３０～１３：５０
研究組織の紹介
研究全般について
「ナノ微粒子体内動態可視化法の開発」

北海道大学大学院歯学研究科生体理工学教室
亘理 文夫

１３：５０～１４：００
「単層カーボンナノチューブ膜での骨芽細胞様細胞の培養」

○赤坂 司[1)]、横山 敦郎[1)]、松岡 真琴[1)]、橋本 剛[3)]
佐藤 義倫[2)]、田路 和幸[2)]、阿部 薫明[1)]、宇尾 基弘[1)]、亘理 文夫[1)]
1) 北海道大学 大学院歯学研究科
2) 東北大学 大学院環境科学研究科
3) 株式会社 名城ナノカーボン

１４：１０～１４：２０
「イメージング質量分析を用いた生体組織観察（3）一水溶性C60の精製ー」

○佐藤 義倫[1)]、久保 拓也[1)]、韮澤 崇[2)]、赤坂 司[3)]、横山 敦郎[3)]、田路 和幸[1)]
1）東北大学 大学院環境科学研究科
2）ブルカー・ダルトニクス（株）
3）北海道大学 大学院歯学研究科

１４：３０～１４：４０
「植物細胞におけるカーボンナノチューブの毒性評価」

○藤井 明洋[1)]、古月 文志[1)]、亘理 文夫[2)]
1）北海道大学大学院環境科学院
2）北海道大学大学院歯学研究科

１４：５０～１５：００
「カーボンナノチューブ複合材料の人工股関節ライナーへの応用」

○大森守[1]・山本剛[1]・橋田俊之[1]・木村久道[2]・大久保昭[2]
東北大学大学院工学研究科[1]・東北大学金研[2]

１５：１０～１５：２０
「チタン合金の水素吸収と諸問題」

徳島大学大学院HBS研究部生体材料工学分野
○淺岡　憲三

１５：３０～１５：５０　　休憩